

## Original Contribution

# Aerial Dispersal and Multiple-Scale Spread of Epidemic Disease

Christopher C. Mundt,<sup>1</sup> Kathryn E. Sackett,<sup>1</sup> LaRae D. Wallace,<sup>1</sup> Christina Cowger,<sup>2</sup> and Joseph P. Dudley<sup>3,4</sup>

<sup>1</sup>Department of Botany and Plant Pathology, Oregon State University, 2082 Cordley Hall, Corvallis, OR 97331

<sup>2</sup>USDA/ARS, Department of Plant Pathology, North Carolina State University, Raleigh, NC 27695

<sup>3</sup>Science Applications International Corporation, 12530 Parklawn Drive, Suite 350, Rockville, MD 20852

<sup>4</sup>Institute of Arctic Biology-University of Alaska Fairbanks, Department of Earth Science, University of Alaska Museum, Fairbanks, AK 99775

**Abstract:** Disease spread has traditionally been described as a traveling wave of constant velocity. However, aerially dispersed pathogens capable of long-distance dispersal often have dispersal gradients with extended tails that could result in acceleration of the epidemic front. We evaluated empirical data with a simple model of disease spread that incorporates logistic growth in time with an inverse power function for dispersal. The scale invariance of the power law dispersal function implies its applicability at any spatial scale; indeed, the model successfully described epidemics ranging over six orders of magnitude, from experimental field plots to continental-scale epidemics of both plant and animal diseases. The distance traveled by epidemic fronts approximately doubled per unit time, velocity increased linearly with distance (slope  $\sim 1/2$ ), and the exponent of the inverse power law was approximately 2. We found that it also may be possible to scale epidemics to account for initial outbreak focus size and the frequency of susceptible hosts. These relationships improve understanding of the geographic spread of emerging diseases, and facilitate the development of methods for predicting and preventing epidemics of plants, animals, and humans caused by pathogens that are capable of long-distance dispersal.

**Key words:** avian influenza H5N1, epidemiology, invasive species, long-distance dispersal (LDD), plant disease, West Nile virus (WNV)

## INTRODUCTION

Infectious diseases and invasive species have important impacts on human health and ecosystem function (Crowl et al., 2008). New pathogens or pathogen strains can spread rapidly, and invasive species often serve as the vectors and/or reservoirs for the establishment of emerging diseases

(e.g., *Culex pipiens* and West Nile Virus; *Aedes albopictus* and dengue). Understanding outbreaks of such diseases can contribute significantly to identifying appropriate disease control strategies (Gewin, 2004). A crucial component of this knowledge is the pattern of disease spread in time and space. Traditionally, disease spread has been modeled as a traveling wave, with constant velocity determined by the reproductive capacity and dispersal ability of a pathogen, and its reservoir host(s) or vector(s) (Mollison, 1977). Epidemic velocity, as defined for purposes of this study, is

Correspondence to: Christopher C. Mundt, e-mail: mundtc@science.oregonstate.edu

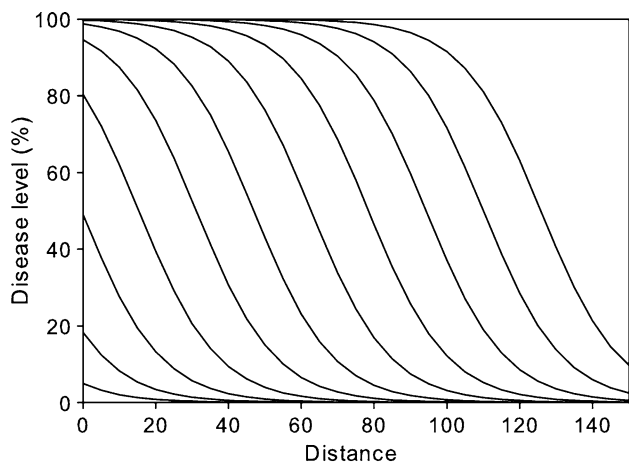


**Figure 1.** Representation of expected disease gradients for a traveling epidemic wave. Data were generated from an integrated form of a spatiotemporal model combining the logistic growth equation for temporal disease increase with a negative exponential for disease spread in space (Eq. [7.33] of Madden et al., 2007). Sequential lines represent disease gradients (disease levels plotted against distance) for observations equally spaced in time.

the distance that the epidemic front advances per unit of time, with the epidemic front defined by either presence/absence of disease or by a specific prevalence level. Traveling wave models are based on random walk processes, with a key assumption that the decline of inoculum with distance, often called a dispersal gradient or dispersal kernel, is exponentially bound (Mollison, 1977). A traveling wave can be represented as a time series of evenly spaced parallel disease gradients moving outward as the epidemic proliferates (Fig. 1).

The form of a pathogen's dispersal gradient strongly affects the expected pattern of disease spread (Kot et al., 1996; Clark et al., 2001; Hastings et al., 2005). A disease that spreads through close proximity or contact between hosts is likely to have an exponentially bound dispersal function and to proliferate as a traveling wave phenomenon (e.g., Grenfell et al., 2001; Cummings et al., 2004). Aerially dispersed pathogens, however, often have dispersal gradients with the extended "fat tails" associated with long-distance dispersal, and the inverse power law has often been used to describe this type of dispersal gradient (Gregory, 1968). Although traveling wave models have sometimes been applied to aerially dispersed plant pathogens, dispersive waves of accelerating velocity may be more appropriate (Ferrandino, 1993; Scherm, 1996; Frantzen and van den Bosch, 2000); many fungal plant pathogens are wind-dispersed, and

long-distance dispersal of spores often dominates their spread (Brown and Hovmøller, 2002). Dispersal of some animal and human pathogens can have a significant aerial dispersal component and, in these cases, may be more accurately described by dispersive wave models (e.g., West Nile virus, foot and mouth disease, and avian influenza).

In this study, we used a simple spatiotemporal model that incorporates the well-known logistic growth equation for the temporal proliferation of disease, and an inverse power law to describe the pathogen's dispersal gradient (Jeger, 1983; Ferrandino, 1993; Madden et al., 2007). The inverse power law as applied to disease is  $y = a/x^b$ , where  $y$  is disease prevalence resulting from pathogen dispersal,  $a$  is the strength of the disease source,  $x$  is distance from the initial disease focus, and  $b$  determines the steepness of the disease gradient. The partial derivatives for this pair of equations yield a prediction for instantaneous epidemic velocity ( $v_t$ ):

$$v_t = rx_t/b \quad (1)$$

where  $r$  is the intrinsic rate of disease increase. A plot of epidemic velocity versus distance should thus give a straight line with slope  $r/b$  if epidemics begin at the same initial distance from the geographic disease focus ( $x_0$ ). A more common comparison of interest would be that of two epidemics expanding from their respective foci at the same time, where,  $x_0$  is proportional to  $r$ , i.e., time is measured in system-specific time units ( $1/r$ ). Velocity can then be described as

$$v_t = x_t/b. \quad (2)$$

Equation (2) is a version of Eq. (1) scaled to account for the fact that initial distance of the epidemic front ( $x_0$ ) is proportional to the infection rate ( $r$ ). Under this function, two epidemics with the same dispersal exponent ( $b$ ) but different infection rate ( $r$ ) will attain the same velocity at a given distance, but it will take the epidemic of lower  $r$  a longer time to arrive at that distance. The position of the wavefront ( $x_t$ ) becomes exponentially more distant from its origin over time (Madden et al., 2007), and can be described (Mundt et al., 2009) as

$$x_t = x_0(b/b - 1)^t. \quad (3)$$

Thus, a plot of  $\ln(x_t)$  versus time should be linear with a slope of  $\ln(b/(b - 1))$ .

We have analyzed the spread of stripe rust (*Puccinia striiformis*), a wind-dispersed fungal pathogen of wheat (*Triticum aestivum*), in artificially inoculated pure and

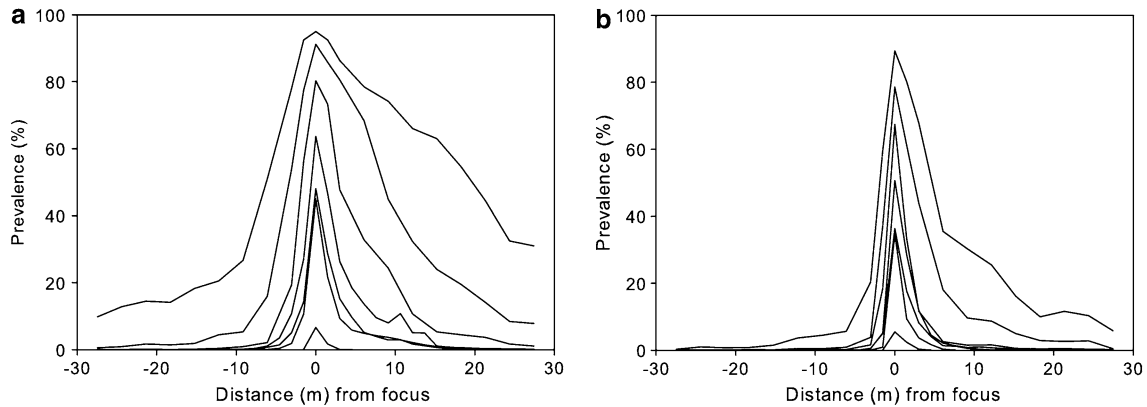


**Figure 2.** Disease gradients of wheat stripe rust in experimental field plots. Prevalence is the percent of the maximum possible number of infections on the susceptible wheat genotype at a given sampling distance. **a** Susceptible wheat genotype in monoculture. **b** Mixture of the susceptible wheat genotype with a resistant one.

mixed plots of wheat genotypes that are either susceptible or resistant to this pathogen. Disease gradients became increasingly flattened over time (Fig. 2), as expected for a dispersive epidemic wave. Wheat stripe rust spread farther in monocultures of a susceptible genotype than in mixed stands of susceptible and resistant wheat genotypes, and farther downwind than upwind (Cowger et al., 2005). To test the validity of Eqs. 2 and 3, we tracked the 30% disease prevalence level in the downwind direction for both monocultures and mixed stands, and found that the position of the epidemic wavefront ( $x_t$ ) became exponentially more distant with time (Fig. 3a). As predicted by Eq. (2), both monoculture and mixed stand data fell on the same line when velocity was plotted against distance (Fig. 3b), but the epidemic wavefront in the mixed stands took longer to reach a given distance than it did in monoculture plots (Fig. 3a). Similar relationships were found among data from all 3 years of the experiment, across multiple prevalence levels, and both upwind and downwind (Mundt et al., 2009).

The power law is scale invariant (Gisiger, 2001), and thus may be applicable across a wide range of spatial scales. To test this hypothesis, we examined the transcontinental spread of five historically important plant and zoonotic disease pandemics: potato late blight, wheat stem rust, southern corn leaf blight, West Nile virus, and H5N1 avian influenza (Mundt et al., 2009). Two of these diseases are explored below.

Potato (*Solanum tuberosum*) late blight, caused by the wind-dispersed oomycete *Phytophthora infestans*, was the proximate cause of the Irish Famine of 1845–1846.

Sequential lines represent disease readings at weekly intervals. Distance 0 represents the site of artificial inoculation; positive distances are downwind and negative distances are upwind. Adapted from Cowger et al. (2005); © 2005, American Phytopathological Society.

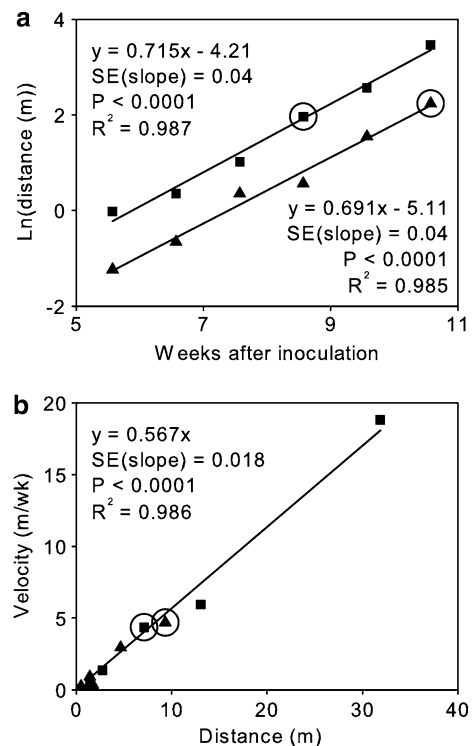


**Figure 3.** Epidemic spread based on 30% disease prevalence of the susceptible wheat genotype for data shown in Fig. 2. **a** Position of epidemic front over time. **b** Epidemic velocity versus distance from initial focus. Squares indicate monoculture population and triangles represent mixture population. Example data points circled in **b** show that epidemic velocity was about 5 m/week at 10 m distance for both monoculture and mixture; comparison with the corresponding points circled in **a** shows that it took the epidemic in the mixture about 2 weeks longer to attain that distance. Adapted from Mundt et al. (2009), © 2009, The University of Chicago Press.

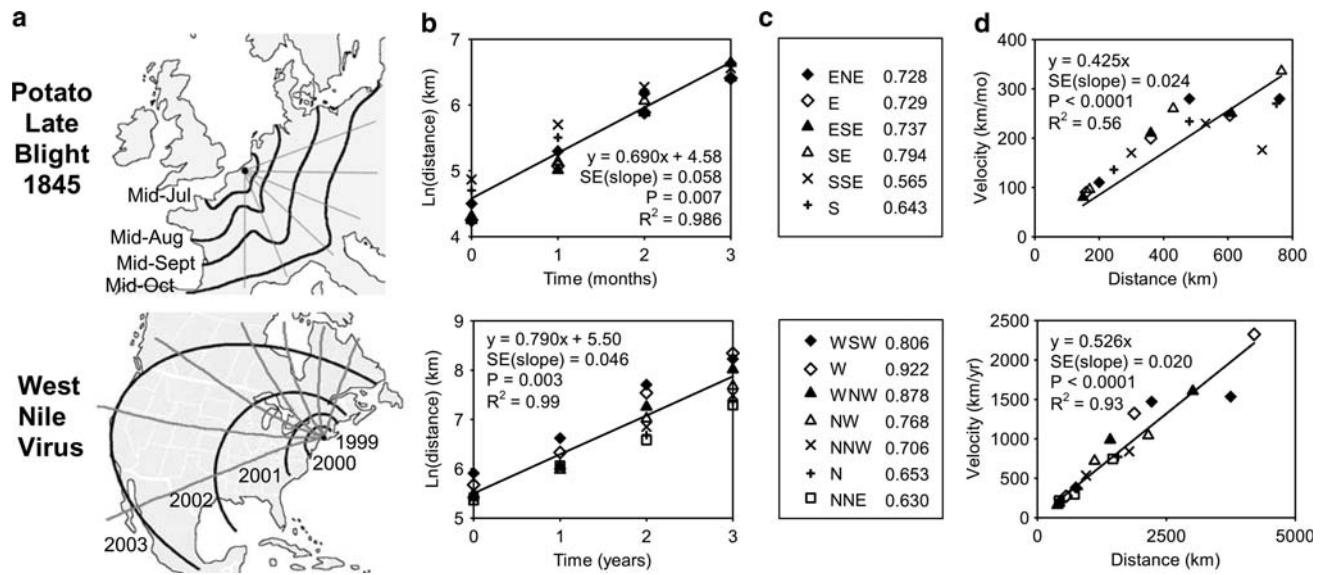


**Figure 4.** Continental spread of potato late blight and West Nile virus. **a** Maps showing original point of introduction (black dot), subsequent spread over time (black curves), and measurement transects (gray lines). **b** Position of epidemic front (log scale) versus time. Regression line is through mean over transect directions. **c** Key for transect directions plotted in **b** and **d**; numbers indicate

regression slopes of  $\ln(\text{distance})$  on time for individual directions. **d** Epidemic velocity versus distance; symbols represent different transect directions. Adapted from Mundt et al. (2009), © 2009, The University of Chicago Press. Map for spread of potato late blight originally adapted from Bourke (1964); used by permission from Macmillan Publishers Ltd, © 1964.

Bourke (1964) retrospectively tracked the path of the epidemic based on accounts in contemporary periodicals, and plotted the position of the epidemic front in monthly increments (Fig. 4a). Using these data, we analyzed the progress of the potato blight epidemic from Belgium (the point of introduction) across continental Europe during the period June through October 1845, along transects separated by 22.5-degree increments (S, SSE, SE, etc.). The observed pattern of this continental-scale epidemic (Fig. 4) matched those from our field-level studies with wheat stripe rust (Fig. 3), i.e., the position of the epidemic front became exponentially more distant with time, and epidemic velocity increased linearly with distance (Fig. 4b–d). There was some deviation from expectation due to both directional and random effects. Overprediction of the regressions for October (Fig. 4b, d) was related mostly to the S and SSE transects, which had the lowest slopes of  $\ln(x_t)$  on time (Fig. 4c) and the largest deviations for the October data in plots of velocity versus distance (Fig. 4d). By October, the epidemic reached the Pyrenees and Alps mountain ranges (and hence the limits of potato production) (Fig. 4a), which restricted its spread in the S and SSE directions. Similar continental spread patterns occurred in North American epidemics of wheat stem rust in 1923 and southern corn leaf blight in 1970 (Mundt et al., 2009).

West Nile virus dispersed rapidly across North America following its initial appearance in New York City in mid-1999, expanding its range through dispersal by migratory birds (Fig. 4a). The epidemic front moved exponentially with time, and velocity increased linearly with distance (Fig. 4b–d). Much of the variation in regression of  $\ln(x_t)$  on time was due to directional effects, which were established early in the epidemic (Fig. 4b). This is supported by the relatively small variation in the regression of velocity on distance (Fig. 4d), for which all data are expected to fall on the same line regardless of  $x_0$ . Though the observed dispersal of West Nile virus was more rapid than predicted by some models (Peterson et al., 2003), the pattern is consistent with predictions from our analysis of empirical data for plant diseases. Avian influenza H5N1, which also is spread in part by migratory birds, exhibited similar behavior in its spread from China across Eurasia and Africa during the period from 2003 to 2006 (Mundt et al., 2009).

The value of  $b$ , the exponent of the power law dispersal gradient, can be estimated from the regression of  $\ln(x_t)$  on time (based on Eq. [3]), or velocity on distance (based on Eq. [2]) (Mundt et al., 2009). Both methods were used with the data shown in Fig. 2 and with five continental-scale epidemics (Mundt et al., 2009). The mean value of  $b$  over

**Table 1.** Estimates of the Exponent,  $b$ , of the Inverse Power Law Dispersal Gradient Required to Obtain Observed Patterns of Disease Spread

Epidemic <sup>a</sup>	Maximum distance (km) <sup>b</sup>	Temporal regressions <sup>c</sup>			Spatial regressions <sup>d</sup>		
		$b$	LCL <sup>e</sup>	UCL	$b$	LCL	UCL
Stripe rust experiment, monoculture	0.032	1.96	1.78	2.21	1.75	1.56	1.98
Stripe rust experiment, mixture	0.009	2.00	1.80	2.29	1.93	1.61	2.41
Potato late blight 1845	700	2.01	1.64	2.81	2.36	2.11	2.67
Stem rust 1923	2180	1.95	1.93	1.96	1.86	1.75	1.99
Southern corn leaf blight 1970	1886	2.14	1.90	2.51	1.96	1.38	3.38
West Nile virus 1999–2002	2563	1.83	1.59	2.24	1.90	1.76	2.06
Avian influenza H5N1 2004–2006	9329	1.74	1.56	2.01	2.05	1.82	2.36
Mean		1.95		1.97			

<sup>a</sup>Data for stripe rust experiments shown in Figs. 2 and 3. Other data shown in Fig. 4 and/or Mundt et al. (2009).

<sup>b</sup>Maximum distance of disease spread observed in each data set.

<sup>c</sup>For temporal analyses,  $b$  was estimated as  $e^s/e^s - 1$ , where  $s$  is the slope of the regression of  $\ln(x_t)$ , position of the epidemic front) on time.

<sup>d</sup>For spatial analyses,  $b$  was estimated as the inverse of the slope of velocity regressed on distance.

<sup>e</sup>LCL and UCL are 95% lower and upper confidence limits of  $b$ , respectively, back-calculated from standard errors of regression slopes.

all regressions of  $\ln(x_t)$  on time was 1.95 (range, 1.74–2.14), the mean value of  $b$  for regressions of velocity on distance was 1.97 (range, 1.75–2.36), and the 95% confidence intervals included 2 in most cases (Table 1). It is therefore reasonable to conclude that an inverse square law may provide a valid approximation for predicting the dispersal rates of aeri ally dispersed pathogens. In fact, an inverse square relationship has been used to describe the dispersal gradients of a range of aeri ally disseminated pathogens, pollen, and seeds (Gregory, 1973; Harper, 1977; Waggoner, 1983; Ferrandino, 1996; Shaw et al., 2006), and bird migration has been described using power law or related “fat-tailed” models (e.g., Paradis et al., 2002; Van Houtan

et al., 2007). Assuming that  $b \sim 2$  provides two simple approximations for the spread of epidemics: the distance of the epidemic front from the initial focus will double per unit time, i.e.,  $x_t = x_0(2)^t$ , and a plot of velocity versus distance will have a slope of  $1/2$ . We evaluated this model at both small (field plot) and large (continental) spatial scales, and expect that it also will be valid at intermediate spatial scales.

The properties of the power law suggest additional scaling relationships for epidemics caused by pathogens capable of long-distance dispersal. For example, a disease governed by power law dispersal should spread in proportion to its initial focus size. To test this, we studied

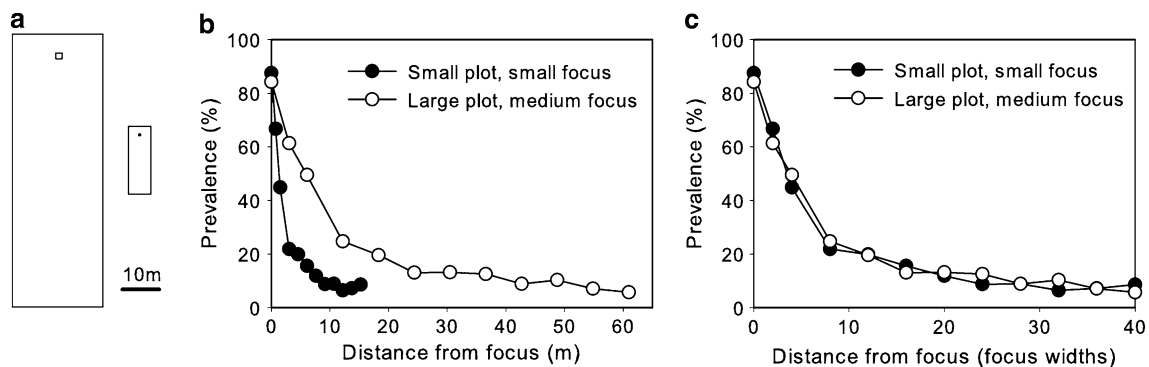


**Figure 5.** Effect of initial disease focus size on epidemic spread of wheat stripe rust. **a** Representation of field plots (rectangles) and artificially inoculated foci (squares within rectangles). Linear dimensions of plots, initial disease foci, and distance between sampling sites

(not shown) in small plots were one-fourth those in large plots. **b** Disease gradient for last sampling date with distance expressed in meters. **c** Same data as in **b**, but distance expressed as number of focus widths.

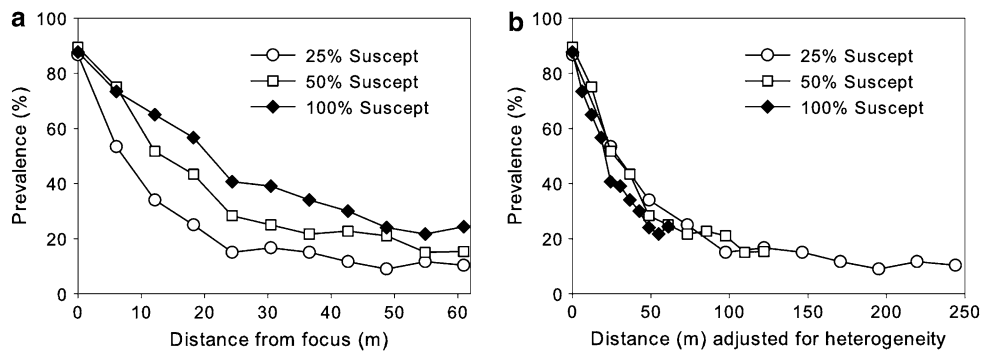


**Figure 6.** Spread of wheat stripe rust in field plots with different percentage of susceptible host plants. Disease prevalence is from readings on susceptible wheat genotypes. **a** Disease gradients for last sampling date with distance expressed in meters. **b** Disease gradients with distance adjusted to percentage of susceptible plants ( $1 \times$ ,  $2 \times$ , and  $4 \times$  distance for 100%, 50%, and 25% susceptible, respectively).

wheat stripe rust in field plots differing in plot and focus size (Fig. 5a). Disease gradients (prevalence plotted vs. distance) show that epidemics advanced substantially farther in plots with larger outbreak foci (Fig. 5b). When scaled to focus width, however, disease gradients were nearly identical, supporting the hypothesis of proportionality to initial focus size (Fig. 5c). We also scaled disease spread to the proportion of susceptible plants in field plots, as the intrinsic rate of disease increase is often expected to be proportional to the frequency of susceptible hosts (Mundt, 2002; Keesing et al., 2006). When disease prevalence was plotted against distance, epidemics advanced farther in plots with a higher proportion of susceptible plants (Fig. 6a). Disease gradients were very similar, however, when prevalence was plotted against distance divided by the proportion of susceptible plants (Fig. 6b). Though yet to be tested, we anticipate that these scaling relationships will apply over a wide range of spatial scales.

Our biogeographic analyses provide simple empirical relationships for predicting and analyzing the spread of pathogens at the field, landscape, and continental scales. The experimental data we evaluated were collected under environmental conditions conducive for disease spread. Deviations from these observed patterns could occur in other conditions, such as when environmental conditions change radically or when spatiotemporal changes in host availability occur (e.g., Aylor, 2003). Our approach is based on data resulting from multiple dispersal events, while predicting individual dispersal events would likely require highly mechanistic meteorological models (e.g., Isard et al., 2005). Further, we expect there to be situations in which epidemic spread is intermediate between dispersive wave and traditional traveling wave models. Despite these

caveats, the empirical evidence we have gathered from recent and historic plant and zoonotic pandemics shows that the properties and patterns they exhibit are similar to those documented in experimental trials (Mundt et al., 2009). The observed parallels and convergences in the spatiotemporal dispersal of pathogens at multiple spatial scales provide a useful heuristic framework for identifying and studying deviations from these expected biogeographic patterns. We believe the relationships we have described can promote a better understanding of the dynamics of the proliferation and geographic dispersal of emerging pathogens, and facilitate the development of improved methods for predicting and preventing epidemics of plants, animals, and humans caused by pathogens capable of long-distance dispersal.

## ACKNOWLEDGEMENT

This work was supported by award 052756 from the NSF/NIH Ecology of Infectious Diseases Program.

## REFERENCES

- Aylor DE (2003) Spread of plant disease on a continental scale: role of aerial dispersal of pathogens. *Ecology* 84:1989–1997
- Bourke PMA (1964) Emergence of potato blight, 1843–1846. *Nature* 203:805–808
- Brown JKM, Hovmøller MS (2002) Aerial dispersal of fungi on the global and continental scales and its consequences for plant disease. *Science* 297:537–541
- Clark JS, Lewis M, Horvath L (2001) Invasion by extremes: population spread with variation in dispersal and reproduction. *American Naturalist* 157:537–554

- Cowger C, Wallace LD, Mundt CC (2005) Velocity of spread of wheat stripe rust epidemics. *Phytopathology* 95:972–982
- Crowl TA, Crist TO, Parmenter RR, Belovsky G, Lugo AE (2008) The spread of invasive species and infectious disease as drivers of ecosystem change. *Frontiers in Ecology and the Environment* 6:238–246
- Cummings DAT, Irizarry RA, Huang NE, Endy TP, Nisalak A, Ungchusak K, et al. (2004) Travelling waves in the occurrence of dengue hemorrhagic fever in Thailand. *Nature* 427:344–347
- Ferrandino FJ (1993) Dispersive epidemic waves: I. Focus expansion within a linear planting. *Phytopathology* 83:795–802
- Ferrandino FJ (1996) Length scale of disease spread: fact or artifact of experimental geometry? *Phytopathology* 86:806–811
- Frantzen J, van den Bosch F (2000) Spread of organisms: can travelling and dispersive waves be distinguished? *Basic and Applied Ecology* 1:83–91
- Gewin V (2004) Disease control: virtual plagues get real. *Nature* 427:774–775
- Gisiger T (2001) Scale invariance in biology: coincidence or footprint of a universal mechanism? *Biological Reviews* 76: 161–209
- Gregory PH (1968) Interpreting plant disease dispersal gradients. *Annual Review of Phytopathology* 6:189–212
- Gregory PH (1973) *The Microbiology of the Atmosphere, 2nd ed.*, London: Leonard Hill
- Grenfell BT, Bjornstad ON, Kappey J (2001) Travelling waves and spatial hierarchies in measles epidemics. *Nature* 414:716–723
- Harper JL (1977) *The Population Biology of Plants*, London: Academic Press
- Hastings A, Cuddington K, Davies KF, Dugaw CJ, Elmendorf S, Freestone A, et al. (2005) The spatial spread of invasions: new developments in theory and evidence. *Ecology Letters* 8:91–101
- Isard SA, Gage SH, Comtois P, Russo JM (2005) Principles of the atmospheric pathway for invasive species applied to soybean rust. *Bioscience* 55:851–861
- Jeger MJ (1983) Analyzing epidemics in time and space. *Plant Pathology* 32:5–11
- Keesing F, Holt RD, Ostfeld RS (2006) Effects of species diversity on disease risk. *Ecology Letters* 9:485–498
- Kot M, Lewis MA, van den Driessche P (1996) Dispersal data and the spread of invading organisms. *Ecology* 77:2027–2042
- Madden LV, Hughes G, van den Bosch F (2007) *The Study of Plant Disease Epidemics*, St. Paul, MN: APS Press
- Mollison D (1977) Spatial contact models for ecological and epidemic spread. *Journal of the Royal Statistical Society. Series B: Statistical Methodology* 39:283–326
- Mundt CC (2002) Use of multiline cultivars and cultivar mixtures for disease management. *Annual Review of Phytopathology* 40:381–410
- Mundt CC, Sackett KE, Wallace LD, Cowger C, Dudley JP (2009) Long distance dispersal and accelerating waves of disease: empirical relationships. *American Naturalist* 173:456–466
- Paradis E, Baillie SR, Sutherland WJ (2002) Modeling large-scale dispersal distances. *Ecological Modelling* 151:279–292
- Peterson AT, Vieglais DA, Andreasen JK (2003) Migratory birds modeled as critical transport agents for West Nile virus in North America. *Vector-Borne Zoonotic Diseases* 3:27–37
- Scherm H (1996) On the velocity of epidemic waves in model plant disease epidemics. *Ecological Modelling* 87:217–222
- Shaw MW, Harwood TD, Wilkinson MJ, Elliott L (2006) Assembling spatially explicit landscape models of pollen and spore dispersal by wind for risk assessment. *Proceedings of the Royal Society of London. Series B: Biological Sciences* 273: 1705–1713
- Van Houtan KS, Pimm SL, Halley JM, Bierregaard RO, Lovejoy TE (2007) Dispersal of Amazonian birds in continuous and fragmented forest. *Ecology Letters* 10:219–229
- Waggoner JE (1983) The aerial dispersal of the pathogens of plant disease. *Philosophical Transactions of the Royal Society of London. Series B: Biological Sciences* 301:451–462